

Double-resonance-enhanced Raman scattering in laser-recrystallized amorphous silicon film

M. C. Lee, C. R. Huang, Y. S. Chang, and Y. F. Chao

*Department of Electrophysics and Institute of Electro-Optical Engineering, National Chiao Tung University,
Hsin Chu, Taiwan 30049, The Republic of China*

(Received 6 April 1989; revised manuscript received 21 July 1989)

Amorphous silicon films after picosecond laser excitation have been investigated by Raman microprobe analysis. The recrystallized Raman peak intensity can be more than four times that of crystalline Si. By carefully examining the annealed microstructure, the enhancement is interpreted as a double-resonance effect due to microcrystals.

I. INTRODUCTION

The laser-induced phase transition in amorphous silicon (*a*-Si) has been extensively studied in recent years for fundamental interests and potential applications.^{1,2} Using laser annealing techniques on *a*-Si thin films,³ we observed that the Raman intensity of the recrystallized peak can be higher than four times that of crystalline silicon (*c*-Si). By taking the Raman intensity ratio of annealed Si to *c*-Si ($I_{\text{annealed}}/I_{c\text{-Si}}$) and tuning the probe wavelength from the visible to the ultraviolet (uv), the Raman enhancement is revealed. This enhancement in the visible (blue-green) region does not appear to be due to the resonance Raman scattering of *c*-Si near the E_{G} and E_1 critical points.⁴ After examining the scanning-electron microscopy (SEM) pictures of picosecond laser excited *a*-Si films, we found that the annealed microstructure is within the range of Mie scattering resonance. However, if we just consider the Mie absorption cross section,^{5,6} the calculated enhancement is not large enough. Because the Raman scattering involves absorption of incident light and scattering of Stokes and anti-Stokes photons, when both the incident and the scattered wavelengths are close to the size of the annealed microcrystals, a double resonance could occur and give rise to the enhancement. Such an interpretation is made since the product of the Mie absorption and scattering cross sections indeed fit our measurements will except in the long-wavelength region which is due to significant interference effects.⁷

II. EXPERIMENT

The details of the film preparation were described in Ref. 3. The film thicknesses are inferred from the spectrophotometric measurements to be 0.8, 1.2, and 1.8 μm , for the 20-, 30-, and 45-min deposition time, respectively. The experimental setup for pulsed-laser annealing and Raman measurements is essentially the same as that in Ref. 8, except a dye laser (PRA LN-107 at 580 nm) of 600 ps was employed. After exciting the *a*-Si films with various fluences from 0.1 to 1.4 J/cm², the microstructure of them was examined under microscope. The Raman intensity was measured by microprobe (10 μm at $1/e^2$) (Ref. 8) at ≈ 2 mW which also serves as a monitor for the local structure variation. All major laser lines from ar-

gon, He-Ne to He-Cd lasers, were employed. The scattered signals were imaged onto a double monochromator (Jobin Yvon U-1000). A multichannel detector (Princeton Instruments (IRY-1024G) was used to increase the signal-to-noise ratio by detecting a wide spectral range for long exposure. For the enhancement analyses, we take the Raman intensity ratio of annealed Si to *c*-Si at each probe wavelength instead of the intensity itself. By doing so, not only the wavelength dependence of the Raman susceptibility and the detection system efficiency can be removed, but the probe power fluctuation is also eliminated. As the result of this normalization, the Raman enhancement is revealed.

III. RESULTS AND DISCUSSION

In Fig. 1, the Raman spectrum of *c*-Si exhibits a strong and sharp peak at 520 cm^{-1} with a linewidth of ~ 3 cm^{-1} , while that of *a*-Si shows a very broad feature (~ 60 cm^{-1}) around 475 cm^{-1} . As the fluence on the *a*-Si is increased to 0.16 J/cm², the broad feature diminishes and a distinct peak emerges at 513 cm^{-1} with a large width. This peak gradually shifts to 518 cm^{-1} with the increasing fluence. It looks similar to that of *c*-Si after 0.38 J/cm². This indicates that the recrystallization volume enlarges with the excitation. However, after excitation ≥ 0.4 J/cm² the Raman-enhancement effect begins to appear. For extracting the enhancement of the recrystallized Raman line, the normalized intensity data obtained by different probe photon energies (they are much larger than the Raman shift) are plotted in Fig. 2 to show whether it is due to the band-gap resonance about 3.4 eV.⁴ When the excitation fluence is increased from 0.3 to 1.2 J/cm², the enhancement peak only slightly shifts from 2.7 to 2.6 eV (457.9 to 476.5 nm). Its profile is sharp around 0.4 J/cm², and becomes broadened above it. This enhancement is obviously not due to the band-gap resonance but to the annealed microstructure of the film.

The detailed structure of three annealed films obtained by SEM are shown in Figs. 3(a)–3(c). The fine crystals formed in thicker films (1.2 and 1.8 μm) are in similar sizes and shapes but the thinnest film (0.8 μm) contains lots of larger crystals. Because the substrate is glass, there is no epitaxial growth. The ball-like particles are mixed in crystalline-amorphous structure. Thus, the

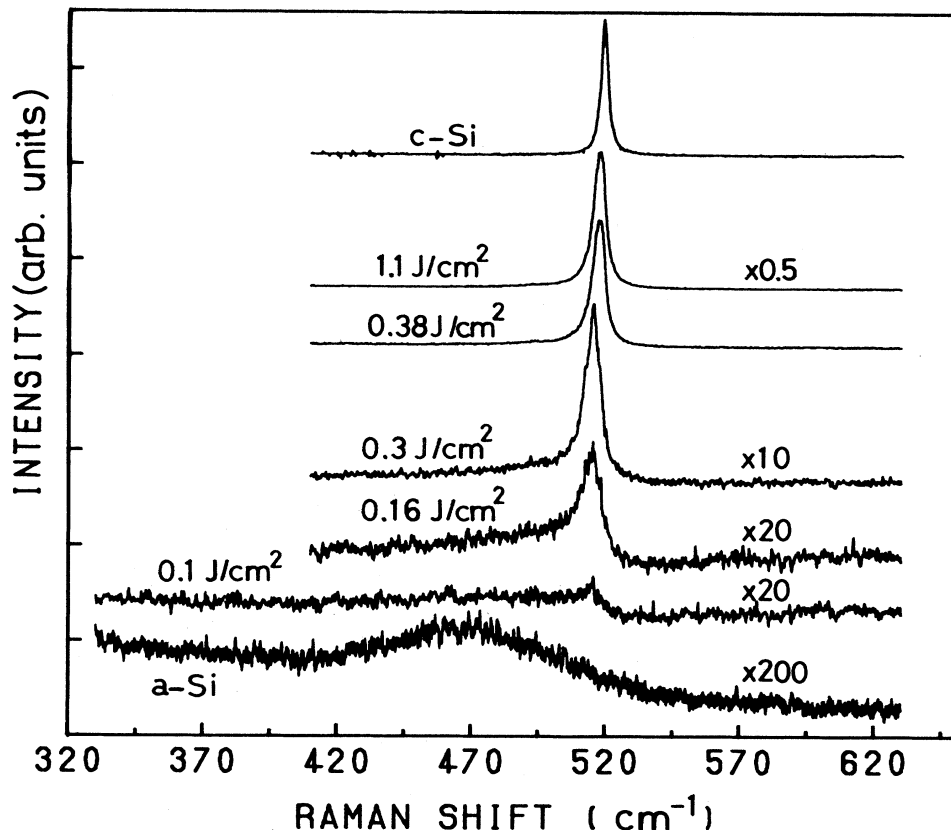


FIG. 1. The Raman spectra of *c*-Si and 1.2- μ m *a*-Si film obtained by 488-nm probe. The recrystallized Raman intensity increases with the fluence that can show the annealing status directly. (\times no.) indicate magnifications.

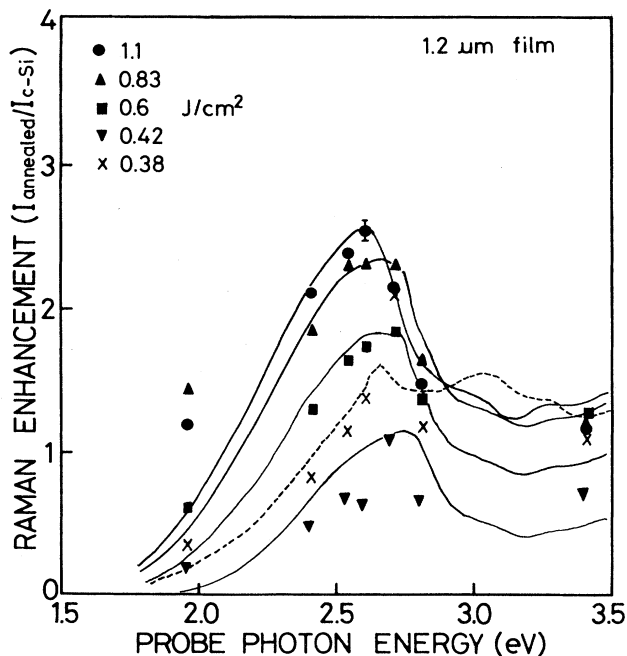


FIG. 2. The Raman enhancement ($I_{\text{annealed}}/I_{c\text{-Si}}$) of 1.2 μ m film after different fluences vs probe photon energy. Solid lines are the calculated $Q_{\text{abs}}Q_{\text{scatt}}$ and the dashed line is the calculated Q_{abs} for 1.1 J/cm², under asymmetric Gaussian distribution.

standard Lorenz-Mie scattering formulas for spherical particles are used to fit the enhancement profile. The normalized efficiency factors of absorption (Q_{abs}) and scattering (Q_{scatt}) cross sections, are given by

$$Q_{\text{abs}} = \frac{1}{2x^2} \sum_{\mu=1}^{\infty} (2\mu+1) [2 - |2a_{\mu}(x, m) - 1|^2 - |2b_{\mu}(x, m) - 1|^2], \quad (1)$$

$$Q_{\text{scatt}} = \frac{2}{x^2} \sum_{\mu=1}^{\infty} (2\mu+1) [|a_{\mu}(x, m)|^2 + |b_{\mu}(x, m)|^2], \quad (2)$$

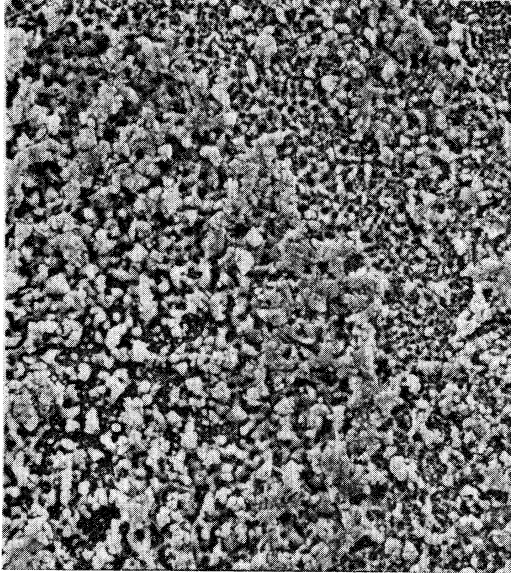
where $x = \pi d / \lambda$ is the size parameter of particle with diameter d , and incident wavelength λ . Due to the optical dispersion of *c*-Si, the corresponding complex refractive indices,⁹ $m = n + ik$, are used to calculate the complex electric and magnetic multipole expansion coefficients of the μ th order (a_{μ} and b_{μ}) in the Mie theory. However, the calculated enhancement for single-particle size is much narrower than what we observed.

Because of rapid nucleation by picosecond laser pulse, the annealed microcrystals are in different sizes. In addition they are not isolated but connected in a porous network as shown in Fig. 3(d), the $\times 10k$ magnification SEM micrograph. The real cause of the network formation is unclear, which may be ascribable to explosive crystallization and its generated shock wave.^{10,11} In order to fit the

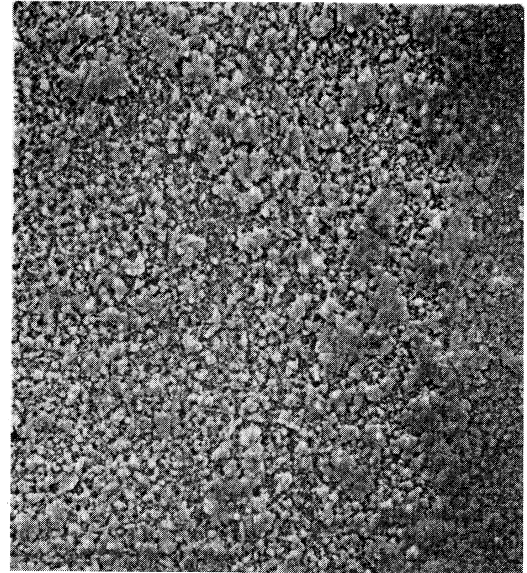
enhancement profile properly, we have to incorporate an asymmetric Gaussian distribution, in which the large and small size deviations $\sigma_1(\sigma_5)$ are introduced besides the mean particle diameter. This assumption of the asymmetric distribution is based on the SEM annealed microstructure and supported by the good fitting to the enhancement. Since recrystallization is more effective from proper crystal size, pulsed annealing should produce unequal size distribution.

Considering the submicrometer crystals as spheres

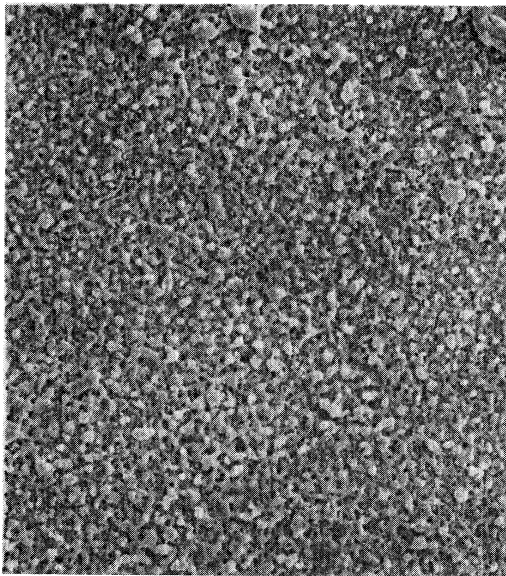
having an asymmetric Gaussian distribution inside the probed region, we find that the calculated Q_{abs} (dashed line in Fig. 2) is not as large as the measured results. Because the Raman process involves absorption of incident light and scattering of Stokes and anti-Stokes photons, a double resonance¹² is suspected. Since the first-order Raman shift of *c*-Si is small compared with the incident photon energy ($\sim 2\%$), when the incident wavelength is close to the particle size for Mie resonance, the scattered wavelength is also near the resonance. Thus, both the incom-



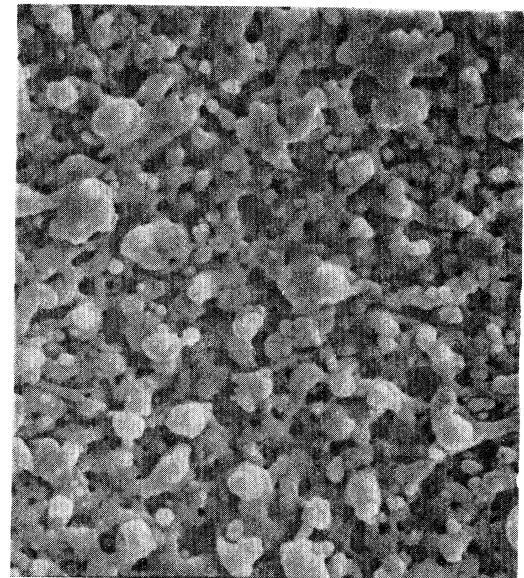
(a)



(b)



(c)



(d)

FIG. 3. SEM micrographs of (a) 0.8-, (b) 1.2-, and (c) 1.8- μm *a*-Si films excited by a 580-nm dye laser (1.1 J/cm^2). There are regions of coarse and fine crystals. (d) Higher magnification of (c), microcrystals are in a porous network.

ing and the outgoing resonances could conceivably occur, giving rise to the enhancement. Taking it in proportion to the product of the Mie absorption and scattering cross sections, several annealed conditions (0.38, to 1.1 J/cm²) are analyzed by choosing (d , σ_1 , and σ_s) from (0.09, 0.03, and 0.01) to (0.1, 0.1, and 0.01) μm . The calculated $Q_{\text{abs}}Q_{\text{scatt}}$ indeed give rise to the resonance in the wavelength domain which are in good agreement with our measurements (solid lines in Fig. 2). Therefore, the microstructure effect is believed to be the cause of the enhanced Raman scattering.

From Fig. 1, the higher Raman intensity results from the stronger excitation which produces the thicker recrystallization layer. For understanding its thickness effect, we only plot the Raman enhancement versus annealing fluence for three different probes in Fig. 4 (all visible probes have similar behavior). As the annealed thickness approaches the probe penetration depth, the enhancement sharply rises about the transition fluence (~ 0.4 J/cm²). Above the transition, large fluctuations are observed in all visible probes but no such variations observed in the uv (363.8 nm) probe. Because the uv photon energy (3.4 eV) is close to the silicon direct gap, due to the strong optical absorption, it is reasonable to estimate the recrystallization thickness to be 300 Å at 0.3 J/cm²; If the Raman cross sections of the annealed film and c-Si are not significantly different, then the effective scattering is inversely proportional to the probe penetration depth. For the thin recrystallized layer (< 0.4 J/cm²), the scattering efficiency of the uv probe is larger than that of the visible probes. This is consistent with the early enhancement rise of the 363.8-nm probe and the low enhancement of the 632.8-nm probe and the low enhancement of the 632.8-nm probe about 0.3 J/cm². However, for the thick recrystallized layer (> 0.4 J/cm²), the large absorption at 363.8 nm eventually suppresses all possible enhancement, so the normalized intensity tails off to 1 (i.e., no enhancement variations). But weak absorption in the long wavelength allows multipole reflection and/or scattering to occur, so that large fluctua-

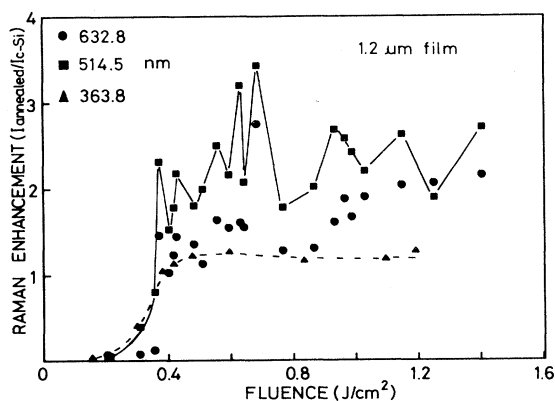


FIG. 4. The Raman enhancement vs annealing fluence. The sharp transition is resulted from a recrystallization layer which is about the probe penetration depth (300 Å at 0.3 J/cm²). Above the transition, the large fluctuations are due to interference.

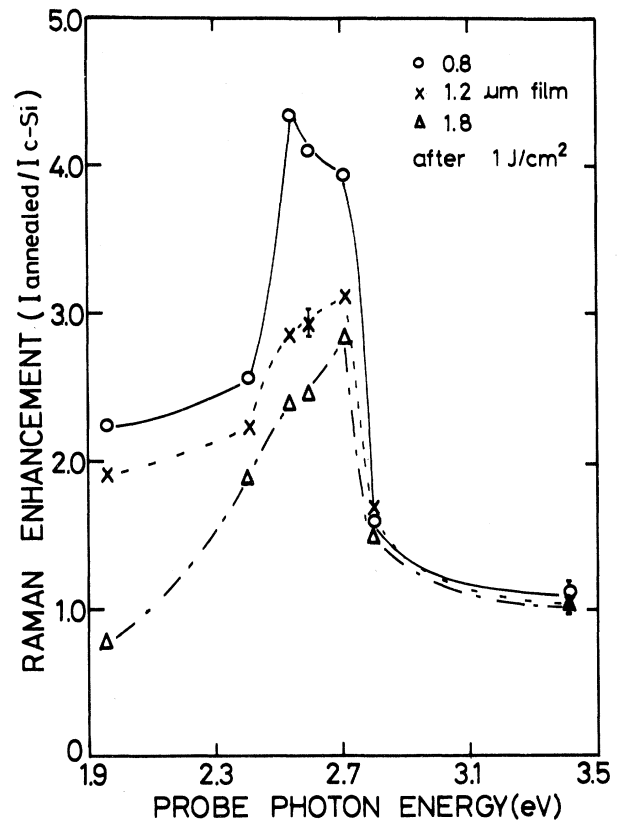


FIG. 5. The Raman enhancement vs probe photon energy. The thinnest film has the largest enhancement. No apparent enhancement beyond 2.8 eV. The large difference below 2 eV is due to interference. Curves are drawn through data points.

tions are observed beyond 0.4 J/cm² for most of the visible probes.

As shown in the SEM pictures, the annealed microstructure is different from one film thickness to another under the same fluence. Since the Raman enhancement is closely related to the annealed microstructure, the results of 0.8-, 1.2-, and 1.8- μm samples are collected in Fig. 5 for comparison. Between 2.4 and 2.8 eV (514.5 to 441.6-nm blue-green region), the largest enhancement appears in the thinnest film and less prominent in the thicker ones. But they all approach unity beyond 2.8 eV, independent of the film thickness. This confirms that strong absorption indeed prevents any enhancing effect. However, the situation below 2 eV is complicated, which can vary from 0.5 to more than 2 as compared with c-Si depending on both the excitation fluence and the film thickness. An interference-enhanced Raman scattering on a relatively transparent multilayer TiO₂/SiO₂ from 570 to 630 nm was observed by Craig *et al.*⁷ Because of weak absorption at 1.96 eV (632.8 nm), the interference effect has to be considered in our experiment to account for the large enhancement variation. Nevertheless, for probe wavelengths between 2.4 and 2.8 eV, the sharp enhancement feature can well be explained by the double-resonance effect from annealed microcrystals.

IV. CONCLUSIONS

Due to the annealed microstructure effect, the Raman enhancement of *a*-Si films is well interpreted as a double resonance by using Mie scattering formulas between 2.4 and 2.8 eV. In long-wavelength probes, the multiple interference effect becomes important and causes intensity variations. However, strong absorption in short wavelengths prevents any enhancement from happening.

ACKNOWLEDGMENTS

We are grateful to Professor Y. C. Lee for his valuable suggestions. We also appreciate Mr. S. Y. Wu for his technical help in taking the SEM pictures. The financial support from the National Science Council of the Republic of China is also acknowledged.

¹*Amorphous Silicon Semiconductors—Pure and Hydrogenated*, Vol. 95 of the *Materials Research Society Proceedings*, edited by A. Madan, M. Thompson, D. Adler, and Y. Hamakawa (MRS, Pittsburgh, PA, 1987).

²M. Bohm, *Solid State Technol.*, September (1988).

³M. C. Lee, C. J. Tseng, C. R. Huang, and T. H. Huang, *Jpn. J. Appl. Phys.* **26**, 193 (1987).

⁴A. Compaan and H. J. Trodahl, *Phys. Rev. B* **29**, 793 (1984).

⁵D. V. Murphy and S. R. J. Brueck, *Opt. Lett.* **8**, 494 (1983).

⁶S. R. J. Brueck, in *Laser Processing and Diagnostics*, Vol. 39 of *Springer Series in Chemical Physics*, edited by D. Bäuerle (Springer-Verlag, Berlin, 1984), p. 446.

⁷R. A. Craig, G. J. Exarhos, W. T. Pawlewicz, and R. E. Willi-

ford, *Appl. Opt.* **26**, 4193 (1987).

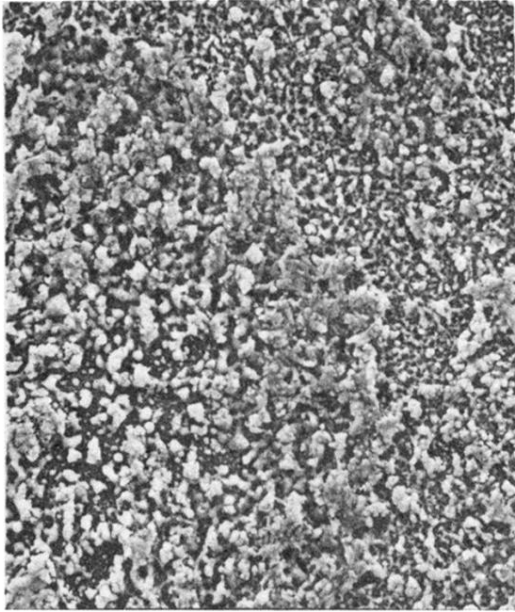
⁸M. C. Lee, C. R. Huang, and C. C. Lin, *Jpn. J. Appl. Phys. Suppl.* **26**, 67 (1987).

⁹D. F. Edwards, in *Handbook of Optical Constants of Solids*, edited by E. D. Palik (Academic, New York, 1985), pp. 547–569.

¹⁰M. O. Thompson, G. J. Galvin, J. W. Mayer, P. S. Peercy, J. M. Poate, D. C. Jacobson, A. G. Cullis, and N. G. Chew, *Phys. Rev. Lett.* **52**, 2360 (1984).

¹¹J. J. P. Bruines, R. P. M. van Hal, B. H. Koek, M. P. A. Vieggers, and H. M. J. Boots, *Appl. Phys. Lett.* **50**, 507 (1987).

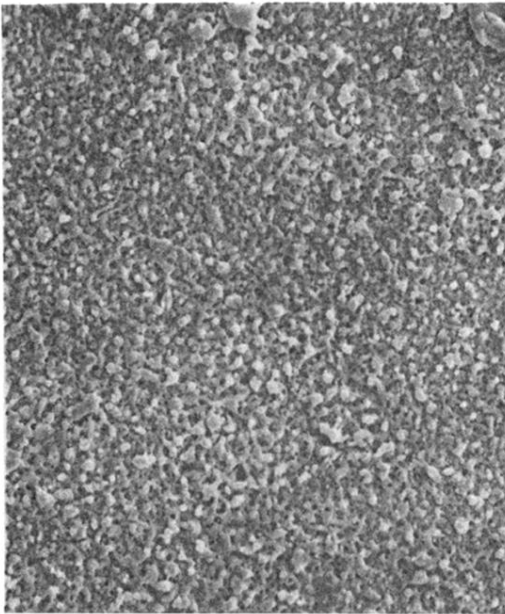
¹²H. Chew and D.-S. Wang, *Phys. Rev. Lett.* **49**, 490 (1982).



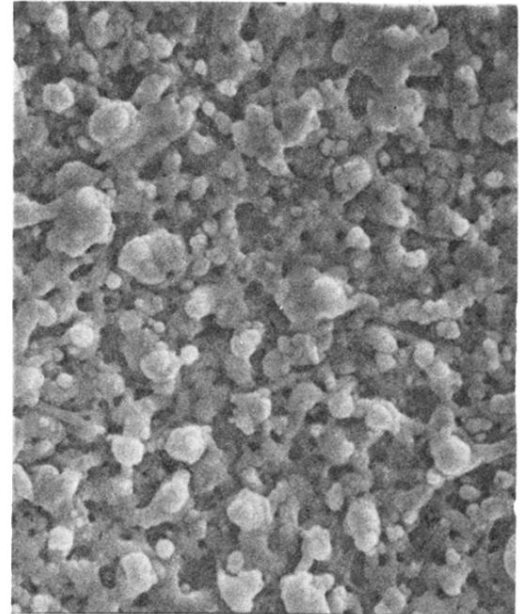
(a)



(b)



(c)



(d)

FIG. 3. SEM micrographs of (a) 0.8-, (b) 1.2-, and (c) 1.8- μm *a*-Si films excited by a 580-nm dye laser ($1.1 \text{ J}/\text{cm}^2$). There are regions of coarse and fine crystals. (d) Higher magnification of (c), microcrystals are in a porous network.